An Analytical Model of Wake Deflection Due to Shear Flow

Daniel Micallef
PhD Student
DUWIND - Delft University Wind Energy Research Institute
Section Wind Energy, Aerospace Faculty, TUDelft Kluyverweg 1, 2629 HS Delft, The Netherlands and University of Malta, Department of Mechanical Engineering, Malta
d.micallef@tudelft.nl

Carlos Simão Ferreira
Researcher
DUWIND - Delft University Wind Energy Research Institute
Section Wind Energy, Aerospace Faculty, TU Delft
Kluyverweg 1, 2629 HS Delft, The Netherlands
c.j.simaoferreira@tudelft.nl

Tonio Sant
Lecturer
University of Malta, Department of Mechanical Engineering, Malta
tonio.sant@um.edu.mt

Gerard van Bussel
Professor
DUWIND - Delft University Wind Energy Research Institute
Section Wind Energy, Aerospace Faculty, TU Delft
Kluyverweg 1, 2629 HS Delft, The Netherlands
G.J.W.vanBussel@tudelft.nl

Abstract

The main motivation behind this work is to create a purely analytical engineering model for wind turbine wake upward deflection due to shear flow, by developing a closed form solution of the velocity field due to an oblique vortex ring.

The effectiveness of the model is evaluated by comparing the results with those of a free-wake model. The solution of the velocity field due to an oblique vortex ring is obtained by using the result of an upright ring along with an equivalent point method. The wake model is derived using oblique ring elements with a number of suitable assumptions. Results of wake vertical deflection are compared with a free-wake solution. A linear trend between wake deflection and shear flow exponent is found with both models. The oblique ring model shows some discrepancies from the free-wake result in terms of the dependence of the deflection on the reference tip speed ratio. The oblique ring model needs further refinements and validation with experimental work and is only currently suited for the determination of general wake kinematics. It however provides immediate results for a given input and can be useful in generating databases with wake geometry information.

Keywords: Horizontal axis wind turbines, Atmospheric shear flow, Vortex rings.

1 Introduction

The horizontal axis wind turbine operates in a shear flow due to the earth's boundary layer, which is detrimental to the overall performance of the machine. A thorough understanding of the aerodynamics of the flow in shear flow is therefore essential. In this work, the wake behaviour of the horizontal axis wind turbine in shear flow is studied.

From two important studies on the near wake physics due to the atmospheric boundary layer [1, 2], the wake was observed to show a slight upward movement. This means that contrary to the case in axial flow conditions, where the wake centerline remains aligned with the wind direction, in the shear flow case, the wake centerline deflects by a small angle.

In the work of Sezer-Uzol et al. [1], a free-wake potential flow panel model was utilized for the situations of 'normal' and 'extreme' wind shear power law profiles, where the National Renewable Energy Laboratory (NREL) Phase VI rotor was simulated. A vertical wake deflection was obtained in the upward direction. In [2], Sørensen et al. performed a similar study but using a numerical simulation of the Reynold's Averaged Navier Stokes Equations (RANS). A difference in tip vortex downstream convection between the top-most and down-most positions of the blade was also observed but the vertical lift of the wake was not all too apparent.

In this work we seek to understand the physical source of the phenomenon, and to derive a closed form model of the wake. This is done by means of vortex rings.

A free-wake, potential lifting line model is first used to simulate the wake in shear flow conditions. To focus mainly on the wake geometry, a 2m diameter flat bladed rotor is modeled.

The results are then used to validate the wake model involving vortex rings.

2 Velocity field due to an upright vortex ring

The details for the analytical solution of an upright, infinitely thin, vortex ring can be found in [3, 4] in the works by Yoon et al. and Nitsche et al. respectively. The analysis of the vortex ring which is presented in this work is based on the Biot-Savart law formulation. The definitions of the variables used here are kept consistent with those found in [3] and are shown in Figure 1.

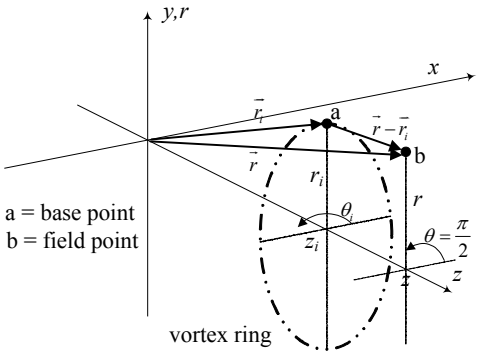

Figure 1: Definition of variables used for the rest of analysis. Source: [3].

From the Biot-Savart law, the velocity vector at any point due to an upright vortex ring is given by equation (1).

$$\vec{u} = \frac{\Gamma}{4\pi} r_i \int_0^{2\pi} \frac{r_i - r\sin\theta_i}{\left|\vec{r} - \vec{r}_i\right|^3} d\theta_i \hat{e}_z + \frac{\Gamma}{4\pi} r_i \int_0^{2\pi} \frac{(z - z_i)\sin\theta_i}{\left|\vec{r} - \vec{r}_i\right|^3} d\theta_i \hat{e}_r \quad (1)$$

Where Γ is the ring circulation, $\hat{e}_z$ and $\hat{e}_r$ are the unit vectors in the axial and radial directions to the ring respectively. Equation (1) reduces to equations (2) and (3) for the velocity component in the axial and radial direction to the ring:

$$u_z = \frac{\Gamma}{4\pi} r_i \left[\left(r_i + r\frac{A}{B} \right) I_2 - \frac{r}{B} I_1 \right] \quad (2)$$

$$u_r = \frac{\Gamma}{4\pi} r_i \frac{z - z_i}{B} \left(I_1 - A I_2 \right) \quad (3)$$

Where $A = (z - z_i)^2 + r^2 + r_i^2$ and $B = -2rr_i$. I_1 and I_2 are given by equations (4) and (5):

$$I_1 = \frac{4}{a} K(m) \quad (4)$$

$$I_2 = \frac{4}{a^3} \frac{E(m)}{1 - m} \quad (5)$$

Where $K(m)$ and $E(m)$ are the complete elliptic integrals of the first and second kind while $m = 4rr_i / a^2$ and $a^2 = (r + r_i)^2 + (z - z_i)^2$.

3 Velocity field due to an oblique vortex ring

3.1 Velocity at the center of the vortex ring

At the center of an oblique vortex ring there should be no radial component of velocity in the coordinate system oriented along the ring. A side view of the ring is shown in Figure 2 which shows the velocity u_z decomposed into v and w in the original coordinate system. The oblique angle of the ring is denoted by β.

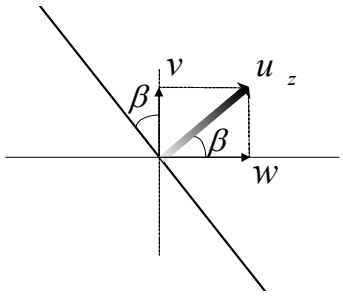

Figure 2: Oblique ring and decomposition of velocity at the center.

The variables from Figure 1 can be defined for this case as $z = z_i = r = 0$, $r_i = R$. Using equation (1), the radial component reduces to 0 as expected while the axial component (z-direction) becomes:

$$u_z = \frac{\Gamma}{4\pi} R \int_0^{2\pi} \frac{R-0}{R^3} d\theta_i$$

$$u_z = \frac{\Gamma R^2}{4\pi R^3}\left[2\pi - 0\right]$$

$$u_z = \frac{\Gamma}{2R} \quad (6)$$

Decomposing into horizontal and vertical components:

$$w = \frac{\Gamma}{2R}\cos\beta \quad (7)$$

$$v = \frac{\Gamma}{2R}\sin\beta \quad (8)$$

3.2 Using the equivalent point method to derive the velocity field

In this work, the model proposed by [3] is extended to include the general situation of an oblique thin vortex ring. The velocity field at any general point other than the centre of the ring cannot be found by simply rotating the velocity components by the oblique angle of the ring. This is because the distance from the point to the perimeter of the thin ring will now change. What is proposed here is to transform the coordinates of a point in the actual domain into an upright vortex ring domain as shown in Figure 3.

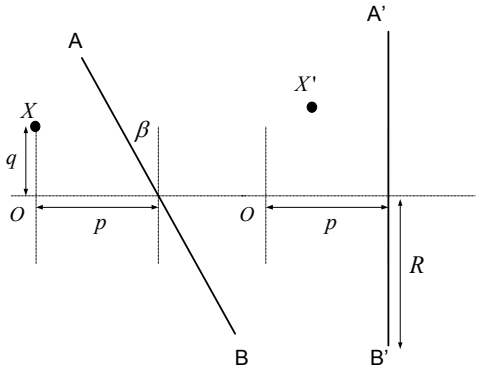

Figure 3: The position of X for an oblique ring (left) corresponds to the position of X' in the upright vortex ring domain (right).

Suppose we need to find the velocity at a point X due to an oblique vortex ring. There must be an equivalent point X' for the upright ring case provided the distances from the perimeter of the ring remain the same as for the oblique ring. The origin is kept the same in both domains which is at a distance p from the centre of the vortex ring. In the oblique vortex ring domain, the position of X is (0,q). In the upright vortex ring domain the position of X' becomes (z'_0, y'_0). The conditions which must therefore be fulfilled are:

$$XA = X'A' \quad (8)$$

$$XB = X'B' \quad (9)$$

To solve this problem, the distance from X' to A' is fixed and is made equal to XA. This condition is satisfied if X' makes a locus about A' which has a fixed distance from A'. This creates a circle, and the objective at this stage is to find a position on the circle such that X'B'=XB. This is shown in Figure 4.

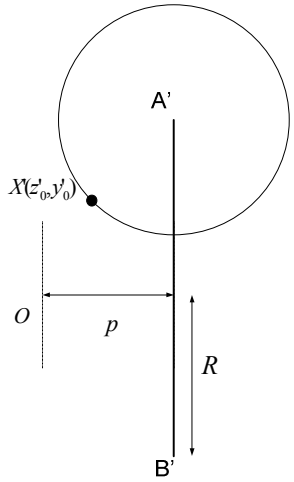

Figure 4: Equivalent point domain with locus of possible positions of X'.

Considering the real point domain we have the following expressions:

$$XA^2 = (R\cos\beta - q)^2 + (p - R\sin\beta)^2 = r_0^2 \quad (10)$$

$$XB^2 = (R\cos\beta + q)^2 + (p + R\sin\beta)^2 = \ell^2 \quad (11)$$

Shifting now to the equivalent point domain the equation for the locus of points at a fixed distance from A' is given by the equation of a circle as follows:

$$(z' - p)^2 + (y' - R)^2 = r_0^2 \quad (12)$$

The condition now is that the distance from B' to the equivalent point which must be found on the circle is equal to ℓ.

$$\left(p - z_0^{'}\right)^2 + \left(y_0^{'} + R\right)^2 = \ell^2 \quad (13)$$

Where the left hand side represents the distance between two points. From equations (12) and (13) $y_0^{'}$ can be found and from equations (10) and (11) simplified to equation (14):

$$y_0^{'} = q\cos\beta + p\sin\beta \quad (14)$$

At the point $\left(z_0^{'}, y_0^{'}\right)$ equation (12) is given by:

$$\left(z_0^{'} - p\right)^2 + \left(y_0^{'} - R\right)^2 = r_0^2 \quad (15)$$

Using (14) in (15):

$$z_0^{'} = p \pm \sqrt{p^2\cos^2\beta + q^2\sin^2\beta - pq\sin 2\beta} \quad (16)$$

The positive value of the square root term of equation (16) is taken.

3.3 Applying the equivalent point method to find the velocity field of an oblique vortex ring

Using the equivalent vortex point method, the velocity at a point due to an oblique vortex ring can be found by using the solution from the upright vortex ring. The situation is depicted in Figure 5.

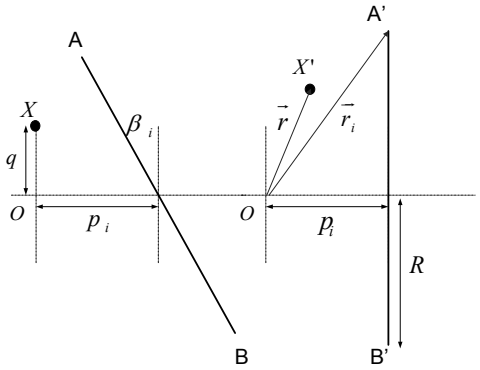

Figure 5: Equivalent point, position vector along with position vector for the base point of the *i*th ring.

The position vector for this *i*th ring is given by:

$$\vec{r}_i = R_i\hat{j} + p_i\hat{k} \quad (17)$$

From equations (15) and (16) the position vector is:

$$\vec{r} = \left(q\ \cos\beta_i + p_i\sin\beta_i\right)\hat{j} + \left(p_i + \sqrt{p_i^2\cos^2\beta_i + q^2\sin^2\beta_i - p_i q\ \sin 2\beta_i}\right)\hat{k} \quad (18)$$

Equations (2) and (3), for an upright vortex ring, may now be applied on the equivalent point to yield the velocity at the required point in the oblique ring domain. The parameters in these equations are hence given by:

$$A_i = p_i^2 + R_i^2 + q^2 \quad (19)$$

$$B_i = -2\left(q\cos\beta + p_i\sin\beta\right)R_i \quad (20)$$

$$a_i = A_i - B_i \quad (21)$$

$$m_i = \frac{-2B_i}{A_i - B_i} \tag{22}$$

$$I_{1,i} = \frac{4}{A_i - B_i} K(m_i) \tag{23}$$

$$I_{2,i} = \frac{4}{(A_i - B_i)^2 (A_i + B_i)} E(m_i) \tag{24}$$

The velocities at the general point due to this *i*th ring are given by:

$$u_{z,i} = \frac{\Gamma_i}{4\pi} r_i \left[\left(r_i + r \frac{A_i}{B_i} \right) I_{2,i} - \frac{r}{B_i} I_{1,i} \right] \tag{25}$$

$$u_{r,i} = \frac{\Gamma_i}{4\pi} r_i \frac{z - z_i}{B_i} \left(I_{1,i} - A_i I_{2,i} \right) \tag{26}$$

These velocities are equal to the velocities found in the oblique ring plane along the axial and radial directions with respect to the oblique ring. Note that if the oblique angle is zero, the solution reduces to the upright vortex ring case and the radial velocity component becomes zero. To obtain the velocities in the horizontal and vertical directions the velocities are simply rotated through an angle β_i:

$$\begin{pmatrix} w_i \\ v_i \end{pmatrix} = \begin{pmatrix} u_{z,i} \\ u_{r,i} \end{pmatrix} \begin{pmatrix} \cos\beta_i & \sin\beta_i \\ -\sin\beta_i & \cos\beta_i \end{pmatrix} \tag{27}$$

This analytical result is also compared with a numerical solution which uses the Biot-Savart law applied to straight line segments forming discretised rings. 10 vortex rings are used for each case. With the numerical simulation, 100 straight line elements are used for each ring. The inclination angle of the rings is taken as 30 degrees for all rings with a pitch and radius of 1m. The velocity at the center of the first ring is calculated and the numerical result agrees with the analytically derived results to 4 decimal places.

4 Wake Model

The infinitely thin vortex ring is a useful tool to simulate wind turbine wakes in a very efficient way. The exact analytical solution to the potential vortex ring problem also allows for a very efficient computation of the induced velocity compared to a spiral wake which requires straight line discretisation. The major drawback is the accuracy of the solution. Emphasis must therefore be made on how these vortex rings are to be configured (their spacing, inclination, strength etc.) in order to obtain a general representation of the flow physics involved. Rather than having a continuous vortex filament, the ring model discretises the continuous spiral into rings which can be considered to be spirals having zero pitch as described by Gupta et al. in [5].

The first important assumption in the oblique ring model (ORM) is that a vortex ring is emanated from the turbine rotor after one complete revolution (see also [5]). The use of thin vortex rings of constant circulation to model the wake was done in the past by Coleman in [6] for the analysis of rotors in forward flight in order to study the azimuthal variation of the induced velocity at the rotor plane. However, the model used by the Coleman employs upright rings, therefore assuming that the wake remains aligned with the flow direction. Indeed, not accounting for lateral induced velocities (as a result of using upright rings) can be considered a flaw in the analysis. Other similar models have been developed by Castles et al. and Young [7, 8]. The developed ORM allows for velocities at the wake centerline to develop such that the wake deflects laterally.

For a two bladed wind turbine, two spirals, 180 degrees out of phase, would therefore be equivalent to one vortex ring (one vortex ring per revolution). The vortex ring has the characteristics of having the radial velocity equal to zero for an upright ring. In axial flow, the wake remains aligned to the flow direction and does not exhibit any deflection. This makes the upright vortex ring particularly suited for such case since in this manner there will be no component of velocity trying to deflect the wake in a particular direction. Since in shear flow the wake was found by Sezer-Uzol et al. to deflect in the vertical direction [1], oblique ring elements may be considered to be best suited.

On the wind turbine site the atmospheric boundary layer will cause sheared inflow and a differential velocity between the topmost and downmost position of the blades will result. This can be used to model the inclination angle of the rings. Figure 6 shows the velocities on the ring

and the definition of the angle of inclination of the ring. In this diagram the maximum and minimum velocities are represented by $u_{\max}$ and $u_{\min}$ respectively. The wind turbine has radius R and it makes one complete revolution in a time Δt. The angle of inclination of the ring is β.

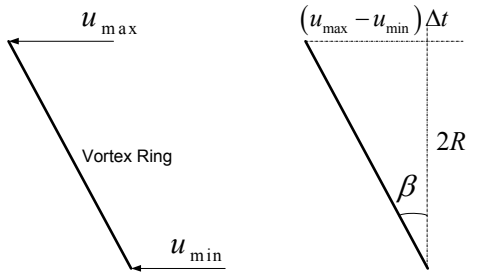

Figure 6: Velocity diagram (left) and corresponding deflection of the ring (right).

The time to make one complete revolution is given by:

$$\Delta t = \frac{60}{\Omega} \tag{28}$$

Where Ω is the rotor rotational speed in RPM. For the *i*th ring the inclination angle is therefore given by:

$$\tan\beta_i = \frac{60i\left(u_{\max} - u_{\min}\right)}{2R\Omega} \tag{29}$$

Writing this in terms of tip speed ratios:

$$\tan\beta_i = \frac{\pi\delta i}{\lambda_{\min}\lambda_{\max}} \tag{30}$$

Where $\delta = \lambda_{\max} - \lambda_{\min}$, $\lambda_{\max}$ is the tip speed ratio when a blade is in its downmost position and $\lambda_{\min}$ is the tip speed ratio when a blade is in its topmost position. The wake model is shown in Figure 7. Due to the oblique rings, a vertical velocity component results, causing the wake to deflect by an angle ζ and a vertical displacement Δs at the origin O.

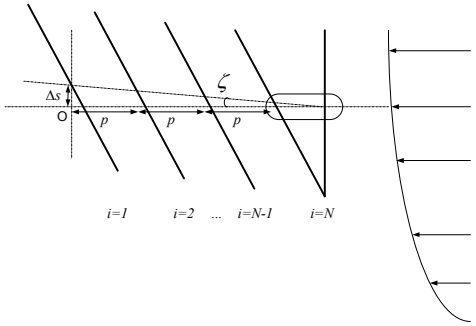

Figure 7: Wake modelled as a ring train.

If the strength of the rings is Γ and the pitch is p then the velocities due to all the N rings, *before* the deflection takes place, are given by:

$$w = \frac{\Gamma_1 \cos\beta_1}{2R_1} + \sum_{i=2}^{N} w_i \tag{31}$$

$$v = \frac{\Gamma_1 \sin\beta_1}{2R_1} + \sum_{i=2}^{N} v_i \tag{32}$$

Of interest for the wake deflection is v. The kinematics of the origin can be described by the integral:

$$\Delta s = \int_0^t v dt \tag{33}$$

If the velocities are assumed to increase in a stepwise manner as they are generated at each revolution (as shown in Figure 8) then the deflection is given by:

$$\Delta s = \Delta t v_N + \Delta t\left(v_N + v_{N-1}\right) + \Delta t\left(v_N + v_{N-1} + v_{N-2}\right) + \cdots + \Delta t\left(\frac{\Gamma_1 \sin\beta_1}{2R_1} + \sum_{i=2}^{N} v_i\right) \tag{34}$$

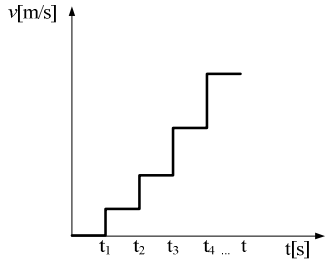

Figure 8: Stepwise increase of velocity at the origin of the wake.

From equation (34) the wake deflection may be found:

$$\tan\zeta = \frac{60N}{(N-1)\Omega p}\left(\frac{\Gamma_1 \sin\beta_1}{2R_1} + \sum_{i=2}^{N} i v_i\right) \qquad (35)$$

The pitch of the rings is assumed to be the distance moved by a ring due to a velocity $U_0(1-a_1)$ in one rotor revolution, where U_0 is the free stream velocity at hub height and a_1 is an assumed averaged induction factor. The expression for the pitch is then:

$$p = \frac{60}{\Omega} U_0 (1-a_1) \qquad (36)$$

Note that this is the distance between each ring center. Due to the variation of the inflow between the top and bottom part of the rotor, the pitches at the top and bottom of the ring will be different. This can be accounted for by changing the inclination angle of the rings β. However the rotor speed in this case is chosen as 720RPM and hence the ring inclinations will be quite small and hence for the revolutions in the very near wake the difference between ring inclinations will also be very small.

The major unknown in this formulation is the circulation of the rings. As an assumption for this initial work, their circulation is assumed to be azimuthally constant and equal to the maximum averaged bound circulation on a blade in one complete revolution. With the current model formulation therefore, no azimuthal variation of circulation is allowed. Nonetheless, each ring itself is the result of an azimuthally averaged condition and in this sense the formulation is consistent. To get an indication of the error which might result with this assumption the variation of the maximum bound circulation with azimuth obtained from the free-wake model is shown in Figure 9. The maximum variation is around 20%. In addition to this, swirl effects are neglected.

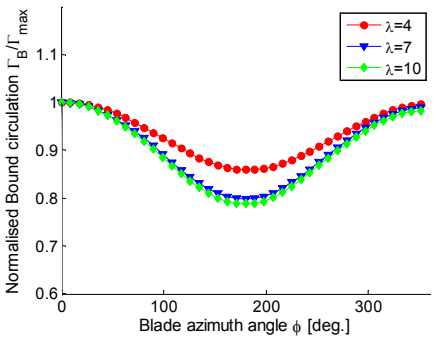

Figure 9: Variation of the maximum bound circulation with azimuth from the free-wake model, with shear exponent set to 0.3.

For the purpose of this study, the maximum bound circulation used for the rings is obtained from the results of a free-wake simulation.

5 Results

5.1 Free-wake results

A lifting line free-wake simulation is performed of a model wind turbine in a sheared inflow. The power law velocity profile is as follows:

$$U(z) = U_0\left(\frac{h}{h_0}\right)^{\alpha} \qquad (37)$$

Where h_0 is the hub height and α is the shear exponent. Table 1 gives the main features of the turbine under investigation.

Table 1 – Model turbine characteristics

Hub height, h_0	2.16 m
Hub radius	0.147 m
Tip radius	1 m
Airfoil	Flat plate

In order to focus on the wake geometry, flat plate blades are used with twist and chord variation as shown in Figure 10. The turbine hub and tower are both ignored and no ground effects are modelled. A total of twelve simulations are performed for combinations of the sets $\alpha = \{0, 0.1, 0.2, 0.3\}$ and $\lambda = \{4, 7, 10\}$ where λ is the tip speed ratio at hub height. The rotor rotational speed is set to 720RPM. The convergence of the results is checked by running additional simulations with different number of span-wise and azimuthal elements and number of rotor

revolutions. For convergence below 4 percent, the number of span-wise elements is taken as 30, azimuthal elements are taken as 40 and 5 rotor revolutions for $\lambda = \{4, 7\}$. For the $\lambda = 10$ case 6 rotor revolutions are used.

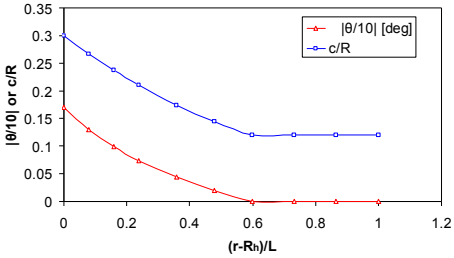

Figure 10: Twist and chord distributions (R_h=hub radius, L=blade length).

The main aim of this work is to obtain information on the deflection of the wake. From the results, the wake deflection observed by Sezer-Uzol et al. [1] is confirmed (Figure 11). This deflection is quantified by assuming that the tip vortex cores are located at the outer edge of the stream tube. A line joining the vortex cores is constructed and the mid-point of each line marked and used as a point on a line whose gradient represents the wake deflection.

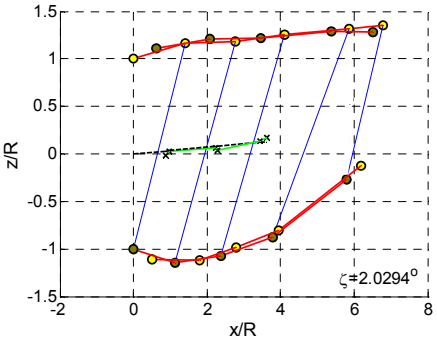

Figure 11: Wake deflection estimation for α=0.2 and λ=4.

5.2 Comparisons with the Oblique Ring Model

The rings are assumed to have radii equal to the rotor radius and hence no wake expansion is modelled. The pitch of successive rings is found from equation (36) with an assumed induction factor of 0.3. The maximum averaged bound circulation is obtained from the free-wake solutions and used in equation (35) for each reference tip speed ratio and shear exponent.

The ORM is a closed form model and allows immediate results to be obtained for various inputs. A large number of results are hence obtained for a large number of shear exponents from 0 to 0.3. The wake deflections from the ORM are compared with those from the free-wake (Figure 12).

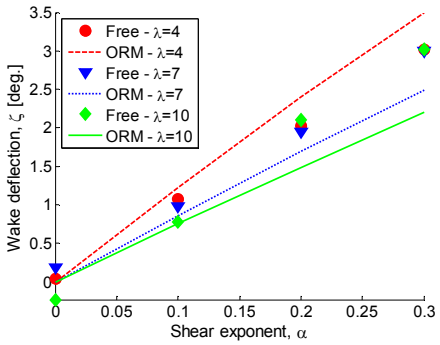

Figure 12: Free-wake and ORM wake deflection results against shear exponent for various tip speed ratios.

Both the free-wake and the ORM results agree in the general linear trend between the wake deflection and the shear exponent. The free-wake results show some very slight deflection when the inflow is non-sheared (uniform, axial flow). Also these show a slight dependence on the tip speed ratio. On the other hand, the ORM gives a higher dependence on the tip speed ratio and the gradient of the lines are quite different from those obtained from the free-wake simulations. With the ORM it is clear that the gradient of the lines increases with decreasing tip speed ratio. Such a trend is not clear with the free-wake results. Experimental results are not yet available for shear flow conditions and hence this dependency on the tip speed ratio is still unclear and needs to be addressed in future work.

6 Potential Uses

Such ring models have been used for hovering and forward flight helicopter rotors as reviewed by Leishman [9]. In the past, Coleman [6] found that the longitudinal coefficient can be expressed as $k_x = \tan(\chi/2)$ for the inflow model for rotors in forward flight with wake skew angle χ.

More recently the Coleman model was used by Chaney et al. [10] for wind turbine applications in order to calculate the centre of thrust for rotors in yawed flow for the purpose of controlling yawing moments on the rotor. Chaney showed that the model results in inflow variation which for yawed flow applications can give 2P variations which resemble more the empirical model of Schepers [11] which was shown to give better results within a BEM approach rather than the simpler Glauert corrections.
These examples are mentioned here to show how such models can provide useful insight of a complicated flow problem. Since the ORM is a purely analytical model, results are obtained instantaneously and wake geometric data may be used for instance in prescribed wake models which may then give more detailed insight of the flow. This potential of the model needs to be carefully assessed.

7 Conclusions

The closed form solution for the velocity field due to an oblique vortex ring is derived from the result of an upright vortex ring. The oblique ring element is used to model the wake of a turbine in shear flow and to obtain a closed form solution to the deflection of the wake due to this sheared inflow.

At this stage, the model requires a suitable input for the ring circulations which in this work is obtained from free-wake simulations of a model turbine rotor. The free-wake results confirm the upward wake deflection observed in [1] and [2] by Sezer-Uzol et al. and Sørensen et al. This is further quantified using the tip vortex positions. Averaged values of circulations are used in the ORM and the deflections compared. The positive aspects of the ORM are:

- The linear trend between wake deflection and shear power law exponent agrees with the free-wake simulations.
- Gives a simple explanation of the physics of the shear flow problem in terms of wake kinematics.
- Can be easily extended to model wake skeweness due to yawed flow.

On the other hand, this analytical solution has various disadvantages:

- Due to the assumptions taken for this model, the detailed flow physics are lacking and only general wake features may be extracted.
- At this stage of the work, the model still relies on various inputs such as ring circulation which are best obtained from experiment or more reliable wake models.
- The dependence on tip speed ratio is different from the free-wake predicted results. This must however still be checked with experimental work.
- The model is not suited to analyse detailed flow physics or to characterize rotor loads.

Future work will address the following issues:

- Experimental work for a turbine in shear flow.
- Extension of the purely analytical model to include more flow physics with the incorporation of rings representing the root vortex.
- Application of model to yawed flow conditions.

8 References

[1] Sezer-Uzol, N., Uzol, O., “Effect of Steady and Transient Wind Shear on the Wake Structure and Performance of a Horizontal Axis Wind Turbine Rotor,” *Proceedings of 47th AIAA Aerospace Sciences Meeting*, 5 - 8 Jan 2009, Orlando World Center Marriott, Orlando, Florida.

[2] Sørensen, N.N. and Johansen J., “UPWIND, Aerodynamics and Aero-Elasticity Rotor Aerodynamics in Atmospheric Shear Flow,” *Proceedings of EWEC 2007*, 7-10 May 2007, Milano Convention Centre, Milan, Italy.

[3] Yoon, S.S. and Heister, S.D., "Analytical formulas for the velocity field induced by an infinitely thin

vortex ring," *Int. J. for Numerical Methods in Fluids,* 2004, 44, 665-672.

[4] Nitsche, M. and Krasny, R., "A numerical study of vortex ring formation at the edge of a circular tube," *J. of Fluid Mechanics*, 1994, 276, 139-161.

[5] Gupta, S. and Leishman J.G., "Accuracy of the induced velocity of wind turbine wakes using vortex segmentation," *Proceedings of 23rd ASME Wind Energy Symposium and 42nd AIAA Aerospace Meeting*, 5 - 8 Jan 2004, Reno, NV.

[6] Coleman, R., Feingold A.M. and Stempin, C.W., "Evaluation of the Induced Velocity Fields of an Idealized Helicopter Rotor," NACA ARR L5E10.

[7] Castles, W., Jr. and De Leeuw, J.H., "The Normal Component of the Induced Velocity in the Vicinity of a Lifting Rotor and Some Examples of Its Application," NACA Report 1184.

[8] Young, C. "The Prediction of Helicopter Rotor Hover Performance Using a Prescribed Wake Analysis," ARC C&P No. 1341.

[9] Leishman J.G., *Principles of Helicopter Aerodynamics*. Cambridge University Press, New York 2006. pp. 607-608. ISBN 978-0-521-85860-1

[10] Chaney K., Eggers A.J., Moriarty P.J., Holley W.E., "Skewed Wake Induction Effects on Thrust Distribution on Small Wind Turbine Rotors," J. Sol. Energy Eng., November 2001, Vol. 123, Issue 4. 290 (6 pages). doi:10.1115/1.1410109.

[11] Schepers J.G., "An Engineering Model for Yawed Conditions, Developed on Basis of Wind Tunnel Measurements", 1999, AIAA-99-0039.

Nomenclature

z [m] = z coordinate of the field point at which the induced velocities are to be calculated.

r [m] = r coordinate of the field point at which the induced velocities are to be calculated.

z_i [m] = z coordinate of the base point on the vortex ring.

r_i [m] = r coordinate of the base point on the vortex ring.

$\vec{r_i} = r_i\hat{e}_r + z_i\hat{e}_z$ [m] = position vector of the field point where the induced velocity is to be calculated.

$\vec{r} = r\hat{e}_r + z\hat{e}_z$ [m] = position vector of the base point on the vortex ring.

$\theta = \pi/2$ [rad] = angle from the horizontal moving anti-clockwise to the field point. The reference angle is taken as 90 degrees.

θ_i = angle from horizontal to the base point.

Γ [m^2/s] = circulation of an infinitely thin vortex ring.

$\vec{u}$ [m/s] = velocity vector at a point due to vortex ring.

$K()$ [-] = complete elliptic integral of the first kind.

$E()$ [-] = complete elliptic integral of the second kind.

u_z [m/s] = velocity component perpendicular to the vortex ring plane at the centre of the ring.

u_r [m/s] = velocity component in the radial direction of the ring.

v [m/s] = vertical component of u_z.

w [m/s] = horizontal component of u_z.

β [deg.] = angle of inclination of the ring.

R [m] = radius of the ring.

$z_0^{'}$ [m] = z coordinate of the equivalent point.

$y_0^{'}$ [m] = y coordinate of the equivalent point.

p [m] = pitch of rings.

q [m] = vertical distance from the origin.

r_0 [m] = distance from a point X to edge A of the ring (see Figure 5).

ℓ [m] = distance from a point X to edge B of the ring (see Figure 5).

$\hat{j}$ [-] = unit vector in the y direction.

$\hat{k}$ [-] = unit vector in the z direction.

$u_{\max}$ [m/s] = wind velocity when the blade is at the top-most position.

$u_{\min}$ [m/s] = wind velocity when the blade is at the down-most position.

Δt [s] = time taken for one rotor revolution.

Ω [RPM] = rotor rotational speed.

$\lambda_{\min}$ [-] = minimum tip speed ratio (top position of blade)

$\lambda_{\max}$ [-] = maximum tip speed ratio (bottom position of blade)

δ [-] = difference between the maximum and minimum tip speed ratio.

ζ [deg.] = deflection angle of wake centerline.

N [-] = number of rings.

Δs [m] = deflection distance of centre of wake at the origin of the wake coordinate system.

t [s] = time.

U_0 [m/s] = free stream velocity at hub height.

a_1 [-] = average axial induction factor.

h_0 [m] = hub height.

h [m] = height from ground.

α [-] = shear exponent.

λ [-] = tip speed ratio.

θ [deg.] = blade twist distribution.

c [m] = blade chord distribution.

R_h [m] = hub radius.

L [m] = blade length.

i (subscript) = ring number.